Acta Ciencia Indica, Vol. XLII P, No. 1, 55 (2016)

S-W POTENTIAL PARAMETERS FOR InN BY AB-INITIO METHODS

S. CHANDRA, POOJA RANI, SARITA MAAN, RANJAN KUMAR

Department of Physics, Punjab University, Chandigarh-160014, India

RECEIVED : 1 March, 2016

REVISED : 28 March, 2016

In this paper we calculate the compliance coefficients and Stillinger-Weber interatomic potential parameters of wurtzite InN by AB-Initio methods. The structural parameters of InN were calculated within the local density approximation of Ceperley-Alder and the generalized gradient approximation of Perdew-Wang exchange-correlation functionals. It was found that the shallow 4*d* electrons were required as part of the valence shell to obtain accurate results due to the large difference in electronegativity between In and N. The calculated compliance parameters were in good agreement with theoretical values and the scattered experimental values. The *AB-Initio* results were then fitted to Stilinger-Weber potential forms.

KEYWORDS : Structural properties, Lattice parameters, S-W parameters.

INTRODUCTION

Wide band gap materials are of special interest for high temperature, high speed transistors, and optoelectronics. Nitrides, in particular, have a high breakdown field and high electron mobilities. Indium nitride has been predicted to have the lowest effective mass among the nitride semiconductors resulting in a high mobility and therefore perhaps has the greatest potential [1-2]. While the growth of InN began over 30 years ago, high quality, single crystalline films have not been achieved, and therefore many of the electrical and physical properties have not been determined with certainty [3]. For example, before 2001 the band gap was thought to be 1.89 eV, now the literature reports experimental values that vary from 0.7 to 2.3 eV for the same wurtzite crystal structure [4-8]. If the mechanical properties of the crystal could be calculated accurately, then large scale dynamic simulation methods such as molecular dynamics method could be used to simulate growth and help predict the growth conditions required to obtain high quality material. This ab-initio method is used for the compliance coefficients of InN and Stillinger-Weber inter-atomic potential parameters.

AB-INITIO METHODS

This computational method is used for structural and elastic properties of InN were performed with the projector augmented wave method within the density functional theory by VASP code [9-10]. Initial trials with only the sp^3 valence electrons proved inaccurate. The

shallow 4*d* electrons were required as part of the valence shell to obtain accurate results due the large difference in electro-negativities between In and N (Phillipsionicity = 0.58). Three structural parameters (lattice constants *a* and *c*, and internal parameter *u*) of wurtzite InN were first calculated by allowing distortions in the shape, volume, and internal coordinates of a four-atom cell with wurtzite symmetry (P6/*mmm*) consisting of two indium and two nitrogen atoms. A wurtzite structure was maintained throughout the distortions. The computations were performed at an energy cutoff of 500 eV with 12 ×12×8 Monkhorst-Pack grids. The atomic positions were relaxed until the forces on the atoms were less than 0.01 eV/A. The structural parameters of InN calculated within the local density approximation (LDA) of Ceperley-Alder and the generalized gradient approximation (GGA) of Perdew-Wang exchange-correlation functionals are listed in Table I along with the experimental values and the results of other calculations. All of the calculated parameters agree well with the experimental data and other theoretical results.

Five different distortions from the theoretically relaxed lattice parameters were considered to calculate the five wurtzite elastic constants C_{11}, C_{12}, C_{13}, C_{33}, and C_{44}. The strain variable (δ) used in the calculation of each elastic constant ranged from -0.02 to 0.02 in steps of 0.002 and otherwise from -0.12 to +0.12 in steps of 0.002 and otherwise from – 0.12 to + 0.12 in steps of 0.01. The calculations involved a full relaxation of the internal degrees of freedom at the same energy cutoff and *k*-points grid as that given above, but the maximum force criterion was reduced to 0.005 eV/Å. The compliance coefficients were fitted to the total energy curves for each distortion, as described in Ashcroft and Mermin [11].

Table I. Wurtzite InN lattice parameters.

	a (Å)	**c (Å)**	**Internal parameter *u***	**Bulk modulus B_M (GPa)**
This work LDA	3.5060	5.6670	0.3768	145
GGA	3.5758	5.7976	0.3762	
Wright *et al.*[a]	3.501	5.669	0.3784	139
Kim *et al.*[b]	3.53	5.54	0.388	
Experiment	3.544[c]	5.718[c]		126[d],139[e]

The strain tensor is defined as a rank 2 symmetric tensor in terms of the primitive vector displacement (e_i) (in reduced notation),

$$\overleftrightarrow{\varepsilon} = \begin{bmatrix} e_1 & 1/2_{e_6} & 1/2_{e_5} \\ 1/2e_{e_6} & e_2 & 1/2_{e_4} \\ 1/2_{e_5} & 1/2_{e_4} & e_3 \end{bmatrix} \quad \ldots (1)$$

Assuming no contribution from heat, the energy is then given by,

$$E(e_i) = E_0 - P(V)\Delta V + V\sum_{i=1}^{6}\sum_{j=1}^{6} 1/2C_{ij}e_i e_j, \quad \ldots (2)$$

where V is the volume of the undistorted lattice, $P(V)$ is the pressure exerted on or by the undistorted lattice at a volume V, and ΔV is the change in volume due to the chosen distortion. The energy of distortion is an even function of distortion since we consider distortions of

sufficiently small amplitude (namely, in the elastic region). This symmetry simplified the above equation by allowing symmetric pressures (tensile and compressional).

The elastic constant combination $C_{11}+C_{12}$ was determined by freezing the lattice parameter c at the theoretical value and distorting $a \rightarrow a' = a\ (1 + \delta)$. To calculate $C_{11} - C_{12}$, we used a volume-conserving distortion with an orthorhombic strain. The elastic constant C_{33} was calculated by keeping the lattice parameter a at the theoretical value and letting $c \rightarrow c' = c(1+\delta)$. The elastic constant combination $C_{11} + C_{12} + 2C_{33} - 4C_{13}$ was calculated by using a volume-conserving distortion with a changed c/a ratio, $a \rightarrow a' = a\ (1 + \delta)$ and $c \rightarrow c' = c/(1+\delta)^2 \approx c\ (1 - 2\delta)$. C_{44} was found by using a volume-conserving monoclinic distortion, for which the energy was an even function of the distortion to all orders. Finally, the bulk modulus was calculated from the computed elastic constants via the expression

$$B_M = \frac{C_{33}(C_{11}+C_{12}) - 2(C_{13})^2}{C_{11}+C_{12}-4C_{13}+2C_{33}} \quad \ldots (3)$$

The value of the bulk modulus obtained from the calculated elastic constants (147 GPa) agrees very well (within 1.3%) with the direct result from the Birch fit to the energy versus volume data [12]. The results of total energy calculations for each distortion are shown in Fig. 1. The region containing densely packed data points in the range $\delta\epsilon$ (– 0.02, 0.02) is the region used to calculate the elastic constants. The total energies from the five different types of distortions for $\delta\epsilon$ (– 0.02, 0.02) were fitted to fifth-order polynomials (without a linear term). The results of the distortions and their corresponding compliance coefficients are given in Table II.

The calculated C_{11}, C_{12}, C_{13}, C_{33}, and C_{44} values are in good agreement with the reported theoretical values and in fair agreement with the experimental datas. In particular, our values for the elastic constants agree quite well with the calculations of Wright [13] . The small differences between the two theoretical works can be attributed to differences in the implemented pseudo-potentials and k-points sampling, which resulted in small variations in the theoretical lattice parameters. To ensure accuracy, this work employed a 500 eV cut-off with a $\{12 \times 12 \times 8\}$ k-point mesh resulting in a = 3.5060 Å, c = 5.6670 Å, and u = 0.3768. u is converging toward the ideal wurtzite parameter of 3/8. The biggest discrepancy between our results and the experimental data is for C_{44}. In order to investigate whether this difference is due to the use of theoretical lattice parameters, we repeated the calculations for C_{44} with the experimental lattice parameters. We used linear terms in the fitting procedure to minimize the energy for these lattice parameters. The value (50 GPa) obtained for C_{44} using the experimental lattice parameters showed no significant difference from the value obtained using the theoretical lattice parameters. The results of all reported *ab-initio* studies vary from the experimental values for C_{33} and, to a lesser degree, for C_{13}. The experimental values largely are imprecise, perhaps due to quality variations in the grown material. This is especially true for the C_{33} coefficient. The calculation of C_{33} involves a uniaxial strain of the c-axis while keeping both a axes fixed. C_{33} and C_{13} have a large experimental uncertainty due to the biaxial strain present in material grown by heteroepitaxy with mismatched lattice constants, which distorts the c axis to maintain approximate volume conservation in Fig. 2. Polytropism in strained InN further modifies the strain properties along the c axis due to the difference between the wurtzite and zinc blende elastic tensor symmetries [14]. The biaxial strain and polytroism may contribute to the observed large variations in experimental values of the energy gap.

The obtained total energy curves were used to fit the InN Stillinger-Weber (SW) potentials with a Levenberg-Marquardt algorithm [15-17]. The SW two-body potential is

similar to a Lennard-Jones potential see in Eq. (5a). Note that the SW potential form also includes a three-body term that simulates directional covalent bonding see in Eq. (5b). To determine approximate values for the potential parameters, a small unit cell (N=27 atoms) was used. This result does not include periodic boundary conditions and as such only gives an initial point to optimize the potential parameters.

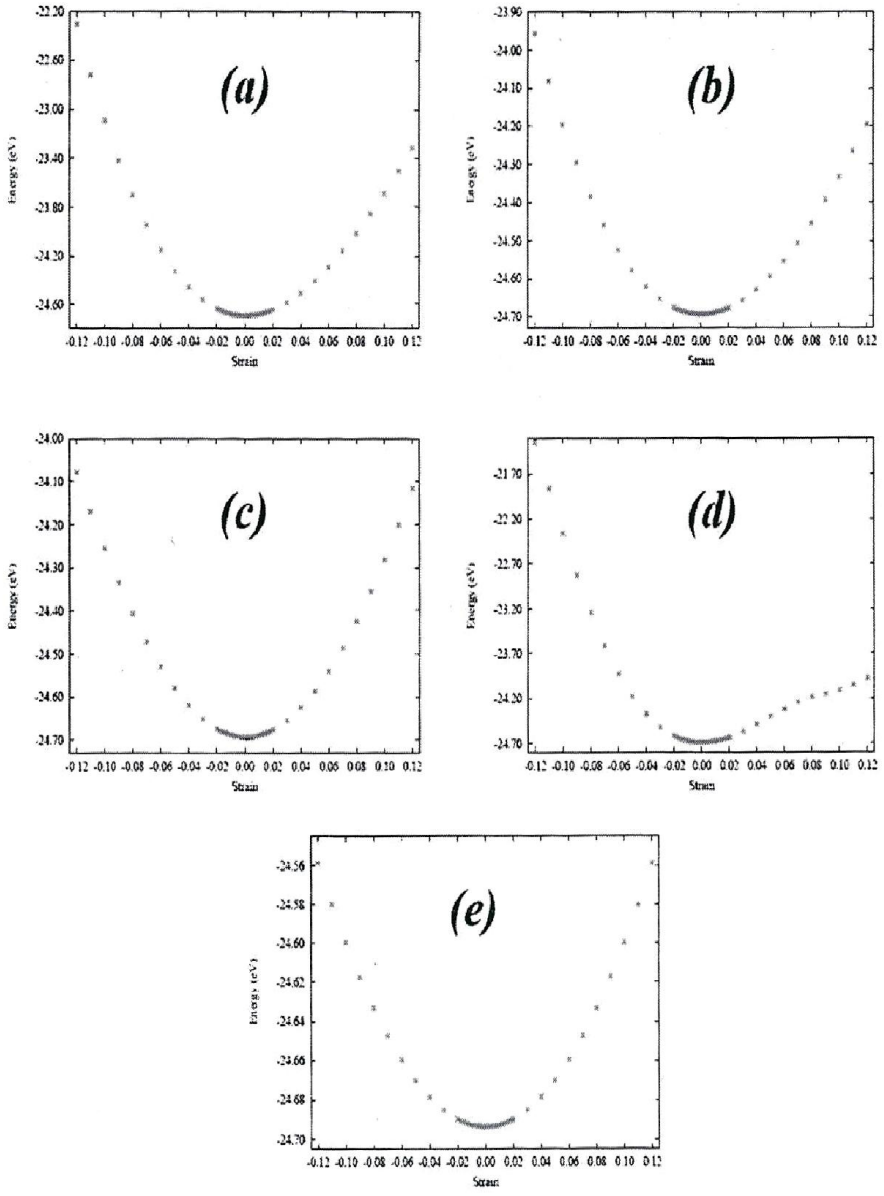

Fig. 1 Calculated values of the total energy for the supercell distortions used in calculating (a) $C_{11}+C_{12}$, (b) $C_{11}-C_{12}$, (c) C_{33}, (d) $C_{11}+C_{12}+2C_{33}-4C_{13}$, and (e) C_{44}.

RESULTS AND DISCUSSION

The average potential energy per atom as given by Stillinger-Weber is

$$\overline{\Phi} = \frac{\sum_{ij}^{i<j} \phi_{ij}^{2-body} + \sum_{i,j,k}^{i<j<k} \phi_{ii,j,k}^{3-body}}{N} \quad \ldots (4)$$

where $\emptyset_{ij}^{2-body} = \varepsilon f^{2-body}(r_{i,j}/\sigma)$ and $\emptyset_{i,j,k}^{3-body} = \varepsilon f^{3-body}(r_i/\sigma, r_j/\sigma, r_k/\sigma)$ such that ε scales f to –1 eV at the minima and σ scales the bond radius such that f_2 ($2^{1/6}$) vanishes ($\sigma = 1.952$ Å). Substitution of the InN vectors $\vec{r}_{ij}$ results in two-and three-body terms that have a seven-dimensional parameter space (A, B, p, q, a, λ, and γ), i.e.

$$f^{2-body}(r) = A(Br^{-p} - r^{-q})\, e^{1/(r-a)} \quad \ldots (5a)$$

and $$f^{3-body}(r_i, r_j, r_k) = h(r_{ij}, r_{ik}, \theta_{jik}) + h(r_{ji}, r_{jk}, \theta_{ijk}) + h(r_{ki}, r_{kj}, \theta_{ikj}) \quad \ldots (5b)$$

where $$h(r_{jj}, r_{ik}, \theta_{jik}) = \lambda e^{[\gamma(r_{ij}-a)^{-1} + \gamma(r_{ik}-a)^{-1}}\, (\cos\theta_{jik} + 1/3)^2 \quad \ldots (5c)$$

Table II. Wurtzite InN elastic constants.

Compliance coefficient (GPa)	AB-Initio result this study	Experiment Sheleg *et al.*[a]	Experiment Wang *et al.*[b]	DFT Kim *et al.*[c]	DFT Wright[d]
C_{11}	229	190±7	223.1	271	223
C_{12}	115	104±3	114.9	124	115
C_{13}	98	121±7	92.0	94	92
C_{33}	240	182±6	221.6	200	224
C_{44}	49	10±1	48.0	46	48
B_M	146.7	139	140.3	147	141

The energy was scaled to the known binding energy (–7.97 eV) divided by the coordination number, 4, for the wurtzite structure. We set $p = 4$ and $q = 1$ to include the ionic nature of InN. The cutoff a and bond angle parameter γ were set to 1.8σ and 1.2σ, respectively. The remaining parameters in the sum (*A, B,* and λ) were fitted to the *AB-Initio* energy curve given in Fig. 2. The distortion changes *c/a* while conserving volume. This changes the strain parameters e_1 and e_2 by $(1 + x)^{1/3} - 1$ and e_3 by $-(1+x)^{2/3} - 1$ where $x = (c/a)/(c/a)_0 - 1$, representing the change in *c/a* from the equilibrium value $(c/a)_0$. This distortion maximizes the three-body contribution to allow for a more accurate determination of λ. The results were rescaled by ε to give the correct bond energy. The resulting three-dimensional parameter space was fitted to the fifth-order polynomial energy curve in Table III.

Table III. Fitted SW parameters for InN.

Parameter	A	B	λ
Value	7.9769	0.7560	15.430

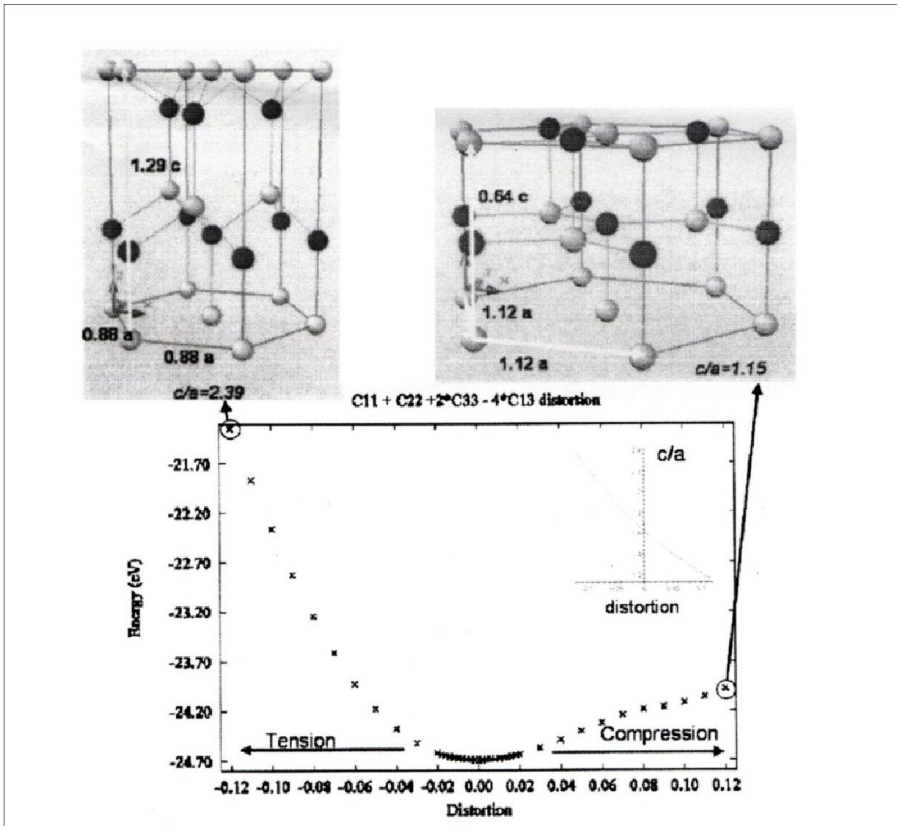

Fig. 2. Volume-conserving $C_{11} + C_{12} + 2C_{33} - 4C_{13}$ distortion. (Upper left) $\delta = -0.12$ distortion, applies a compression on *a* and tension on *c*. (Upper right) $\delta = 0.12$ distortion, compression on c and tension on a. (Bottom) Computed energy as a function of distortion. The inset plots *c/a* as a function of distortion.

Conclusion

AB-Initio methods was used to calculate the compliance coefficients of InN through a series of five distortions. The total energy curves were scaled and fitted to determinate the SW potential parameters. It was determined that the $1/r$ term in the SW potential is large so that the ionic character of InN is significant and thus the $3d^{10}$ shell must be included in the *AB-Initio* calculation. The compliance coefficients agree with experiment with the exception of the C_{33} parameter. This parameter is substantially affected by the biaxial strains created during growth and by laminar polytropism, and thus has a large experimental uncertainty.

Acknowledgement

This work is supported by University Grants Commission, New Delhi (Grant No.PDFSS-2011-12-SC-UTT-2848), India. The authors are thankful to Prof. Jai Shanker, Department of Physics, Institute of Basic Science, Khandari Campus, Agra.

REFERENCES

1. Mohammad, S. N. and Morkoç, H.. *Prog. Quantum Electron*., **20**, 361 (1996).
2. Bhuiyan, A. G., Hashimoto, A. and Yamamoto, A., *J. Appl. Phys*., **94**. 2779 (2003).
3. Hovel, H. J. and Cuomo, J. J., *Appl. Phys. Lett*., **20**, 71 (1972).
4. Tansley, T. L. and Foley, C. P., *J. Appl. Phys.*, **59**, 3241 (1986).
5. Davydov, V. Y., *et. al., Proc. SPIE,* **5023**, 68 (2003).
6. Matsuoka, T., Okamoto, H., Nakao, M., Harima, H. and Kurimoto, E., *Appl. Phys. Lett*., **81**, 1246 (2002).
7. Wu, J., Walukiewicz, W., Yu, K. M., Ager, J. W. III, Haller, E. E., Lu, H., Schaff, W. J., Saito, Y. and Nanishi, Y., *Appl. Phys. Lett*., **80**, 3967 (2002).
8. Butcher, K. S. A. and Tansley, T. L., *Superlattices Microstruct*., **38**, 37 (2005).
9. Blöch, P. E., *Phys. Rev*., B **50**, 17953 (1994).
10. Kresse, G. and Hafner, J., *Phys. Rev*., B **47**, R558 (1993).
11. Ashcroft, N. and Mermin, N., *Solid State Physics,* **1st ed.**, Brooks Cole (1976).
12. Birch, F., *J. Geophys. Res*., **83**, 1257 (1978).
13. Wright, A. F. and Nelson, J. S., *Phys. Rev*., B **51**, 7866 (1995).
14. Muñoz, A. and Junc, K., *J. Phys.: Condens. Matter*, **5**, 6015 (1993).
15. Stillinger, F. H. and Weber, T. A., *Phys. Rev*., B **31**, 5262 (1985).
16. Levenberg, K., *Q. Appl. Math.*, **2**, 164 (1944).
17. Marquardt, D., *J. Soc. Ind. Appl. Math*., **11**, 431 (1963).
18. Kim, K. W., Lambrecht, R. L. and Segall, B., *Phys. Rev*., B **53**, 16310 (1996).
19. Osamura, K., Naka, S. and Murakami, Y., *J. Appl. Phys*., **46**, 3432 (1975).
20. Ueno, M., Yoshida, M., Onodera, A., Shimomura, O. and K. Takemura, *Phys. Rev*., B **49**, 14 (1994).
21. Sheleg, A. and Savastenko, V. A., Izv., Akad., Nauk, S.S.S.R., *Neorg. Mater.*, **15,** 1598 (1979) [*Inorg. Mater*., **15**, 1257 (1979)].
22. Wang, K. and Reeber, R. R., *Appl. Phys. Lett*., **79**, 1602 (2001).
23. Kim, K., Lambrecht, R. L. and Segall, B., *Phys. Rev*., B **50**, 1502 (1994).
24. Wright, A. F., *J. Appl. Phys*., **82**, 2833 (1997).

❑